Supplement of Atmos. Chem. Phys., 24, 5847–5862, 2024
https://doi.org/10.5194/acp-24-5847-2024-supplement

Atmospheric Chemistry and Physics
Open Access

Supplement of

Role of sea spray aerosol at the air–sea interface in transporting aromatic acids to the atmosphere

Yaru Song et al.

Correspondence to: Lin Du (lindu@sdu.edu.cn)

Table of contents

List of tables

List of figures

S1. Quality assurance/quality control

Seawater was collected from the coastal area of Shazikou on March 27, 2023, with a volume of 500 L (Fig. S1). Considering the storage inconvenience caused by huge consumption of seawater, all our seawater was pre-filtered through a polyethersulfone filter (47 mm diameter, 0.2 μm pore size, Supor®-200, Pall Life Sciences, USA) and stored in the dark at 18 ℃ for less than one month. Quinn et al. (2015) have shown that the fraction that passes through the filter is regarded as dissolved organic carbon and includes colloidal and truly dissolved materials. For each experiment, we measured particle number concentrations generated by filtered seawater and cations concentrations in seawater, and we found good agreement between each set of experiments (see Fig. S2).

In order to avoid the influence of organic matter in quartz fiber filters and access the accuracy of the experiment, pre-baked quartz fiber filters were used in sampling. Before each set of experiments, experimental blanks were conducted using filtered seawater. Experimental blanks were conducted with the same procedure of SSA samples. Seawater and filter samples were stored at -20°C until analyzed. In order to reduce the influence of organic acids residue after each experiment, the SSA simulation chamber was cleaned with ethanol first, then the system was cleaned with ultra-pure water for several times. The above steps also run the pump to allow for thorough cleaning of the system. Thereafter, the system was blown with zero air and sealed for preservation. The Dekati DLPI was also ultrasonicated with methanol and water (V:V=1:1) and dried after the experiment.

Filtered seawater (without added aromatic acid) was used as the experimental blank, and the same experimental and analytical methods were used as those for the experimental samples. As a result, no target aromatic acid was found in both seawater and filters. This may be due to the fact that we did not perform any concentration operation during the sample processing. The standard curves for each aromatic acid are linear, as shown in Fig. S5.

Table S1. Sources and concentrations of aromatic acids identified in seawater and atmospheric samples over the ocean.

Aromatic acids	**Natural sources**	**Anthropogenic sources**
benzoic acid	● sea algae (Abdel-Hamid A. Hamdy, 2020; Al-Zereini et al., 2010; Fotso Fondja Yao et al., 2010; Liu et al., 2022) ● sedimentary organic matter (10–65 μg g^{-1}) (Deshmukh et al., 2016) ● bacteria isolated from sea bass viscera (0.3 μM) (Martí-Quijal et al., 2020) ● snow pit samples (2.11 ng g^{-1}) (Mochizuki et al., 2016)	● emerging endocrine disrupting compounds (0.3–4.0 nM) (Zhao et al., 2019) ● fuel combustion (Boreddy et al., 2017) ● industrial wastewater, automobile exhaust and tobacco smoke (Cuadros-Orellana et al., 2006)
o-phthalic acid		● plasticizer (16.7–657 ng g^{-1} d.w.) (Ren et al., 2023; Sanjuan et al., 2023) ● plastic waste burning (8.3–84.9 ng m^{-3}) (Zhu et al., 2022) ● the end product of photochemical oxidation of SOA (15.5 ng m^{-3}) (Ding et al., 2021) ● biomass burning and fossil fuel combustion sources (0.4–7.9 ng m^{-3}) (Shumilina et al., 2023; Yang et al., 2020; Boreddy et al., 2022)

m-phthalic acid		● plasticizer (Ren et al., 2023) ● the end product of photochemical oxidation of SOA (3.6 ng m^{-3}) (Ding et al., 2021) ● biomass burning and fossil fuel combustion sources (0.01–2.3 ng m^{-3}) (Yang et al., 2020; Boreddy et al., 2022; Kawamur, 2014)
p-phthalic acid		● plasticizer (0.51–6.8 mg kg^{-1}) (Ren et al., 2023; Di Giacinto et al., 2023; Di Renzo et al., 2021) ● plastic waste burning (10.8–80.7 ng m^{-3}) (Zhu et al., 2022); the end product of photochemical oxidation of SOA (4.3 ng m^{-3}) (Ding et al., 2021) ● biomass burning and fossil fuel combustion sources (0.05–2.5 ng m^{-3}) (Yang et al., 2020; Boreddy et al., 2022; Kawamur, 2014)
o-hydroxybenzoic acid	● sea algae (0.5 mM) (Castillo et al., 2023; Mostafa et al., 2017; Klejdus et al., 2017)	● pharmaceuticals and drugs of abuse (2.8–385.9 pM) (Alygizakis et al., 2016)
m-hydroxybenzoic acid	● sea algae (Al-Zereini et al., 2010; Castillo et al., 2023)	

p-hydroxybenzoic acid	● sea algae (0.4 mM) (Castillo et al., 2023; Klejdus et al., 2017; Tian et al., 2012; Hawas and Abou El-Kassem, 2017) ● sea fungus (Rukachaisirikul et al., 2010; Shao et al., 2007) ● sponge Mycale species (Zhou et al., 2013); metabolite (Jingchuan Xue, 2015; Liao and Kannan, 2018) ● sediment samples (6.85–437 ng g^{-1} dw) (Liao et al., 2019)	● Pharmaceuticals and personal care products (Lu et al., 2023) ● emerging endocrine disrupting compounds (0.03–0.4 nM) (Zhao et al., 2019; Lu et al., 2021; Alygizakis et al., 2016)
vanillic acid	● sea algae (0.02–0.3 nM) (Zangrando et al., 2019; Klejdus et al., 2017) ● lignin decomposition (Wang et al., 2015; Hu et al., 2022; Xu et al., 2017)	● combustion of both softwood and hardwood (Simoneit, 2022)
syringic acid	● sea algae (1.5–3 pM) (Poznyakovsky et al., 2021; Zangrando et al., 2019; Klejdus et al., 2017) ● lignin decomposition (Hu et al., 2022; Xu et al., 2017)	● pharmaceuticals (Fisch et al., 2017) ● hardwood burning (Simoneit, 2022)

Table S2. Dimensions and operating conditions of the SSA simulation chamber.

Characteristic	Value
Nozzle diameter (mm)	4.3
Seawater depth (cm)	15
Seawater volume (L)	9
Headspace depth (cm)	22
Headspace volume (L)	15
Zero sweep air (L min^{-1})	3
Headspace residence time (min)	5
Plunging jet flow rate (L min^{-1})	1

Table S3. Summary of experimental conditions.

Exp. No.	Experiment type	Concentration (mM)	pH	Salinity (psu)	Sampling time (h)	RH (%)	Temperature difference (℃) [a]
1	SW	0	7.92	34.2	5	35	2.0
2	SW+benzoic acid	1	7.72	34.3	5	34	1.5
3	SW+*o*-hydroxybenzoic acid	1	7.60	34.5	5	36	1.0
4	SW+*m*-hydroxybenzoic acid	1	7.68	34.1	5	40	2.0
5	SW+*p*-hydroxybenzoic acid	1	7.84	34.3	5	38	1.5
6	SW+*o*-phthalic acid	1	7.58	34.2	5	36	2.0
7	SW+*m*-phthalic acid	1	7.80	34.5	5	37	2.5
8	SW+*p*-phthalic acid	1	7.85	34.4	5	42	2.0
9	SW+vanillic acid	1	7.81	34.2	5	43	3.0
10	SW+syringic acid	1	7.84	34.3	5	39	2.0
11	ASW	0	7.96	35.1	5	33	1.5
12	ASW+benzoic acid	1	7.68	34.6	5	35	1.0
13	ASW+*o*-hydroxybenzoic acid	1	7.76	34.9	5	34	0.5
14	ASW+*m*-hydroxybenzoic acid	1	7.99	35.3	5	36	1.5
15	ASW+*p*-hydroxybenzoic acid	1	7.85	34.7	5	38	2.0
16	ASW+*o*-phthalic acid	1	7.93	34.5	5	35	1.0

17	ASW+*m*-phthalic acid	1	7.88	34.9	5	36	1.0
18	ASW+*p*-phthalic acid	1	7.97	34.6	5	34	1.5
19	ASW+vanillic acid	1	7.89	35.2	5	35	1.0
20	ASW+syringic acid	1	7.99	34.8	5	39	1.0
21	ASW+benzoic acid+*o*-hydroxybenzoic acid+*o*-phthalic acid+vanillic acid+syringic acid	10^{-3}	7.95	35.1	20	41	3.5
22	ASW+benzoic acid+*m*-hydroxybenzoic acid+*m*-phthalic acid+vanillic acid+syringic acid	10^{-3}	7.98	34.6	20	38	1.5
23	ASW+benzoic acid+*p*-hydroxybenzoic acid+*p*-phthalic acid+vanillic acid+syringic acid	10^{-3}	7.88	34.9	20	40	2.0
24	NaCl	0	7.68	35.3	5	38	1.0
25	NaCl+*m*-hydroxybenzoic acid	1	7.54	34.7	5	36	1.5

[a] The temperature difference in the SSA simulation chamber before and after the experiment.

Table S4. Octanol−water partitioning coefficients log(*K*ow) and octanol−air partitioning coefficients log(*K*oa) of aromatic carboxylic acids.

aromatic carboxylic acids	**log(*K*ow)**	**log(*K*oa)**
benzoic acid	1.87	5.91
o-hydroxybenzoic acid	2.26	7.44
m-hydroxybenzoic acid	1.5	8.08
p-hydroxybenzoic acid	1.58	8.08
o-phthalic acid	0.73	7.84
m-phthalic acid	1.66	7.84
p-phthalic acid	2	7.84
vanillic acid	1.43	7.84
syringic acid	1.04	7.95

Table S5. Aromatic acid concentration in seawater and estimated value k_{SSA}.

	Aromatic acid concentration in seawater (ng L^{-1})			k_{SSA} (pg μg^{-1})		
	low	medium	high	low	medium	high
benzoic acid	34	205	491	0.0235	0.142	0.304
o-hydroxybenzoic acid	0.4	-	53.3	0.0002	-	0.026
m-hydroxybenzoic acid	-	-	-	-	-	-
p-hydroxybenzoic acid	4.58	8.66	49.9	0.004	0.008	0.044
o-phthalic acid	-	-	-	-	-	-
m-phthalic acid	-	-	-	-	-	-
p-phthalic acid	-	-	-	-	-	-
vanillic acid	3	-	47	0.04	-	0.623
syringic acid	0.3	-	0.6	0.007	-	0.015

Table S6. Estimated annual global aromatic acids emission (tons yr^{-1}) via SSA.

		SSA emission based on Textor et al. (2006) (10^{12} kg yr^{-1})			SSA emission based on Gliss et al. (2021) (10^{12} kg yr^{-1})		
		3.65	6.25	9.7	3.65	4.98	6.62
		Global aromatic acids emission (tons yr^{-1})					
benzoic acid	low	27	45	71	27	36	48
benzoic acid	medium	161	275	427	161	219	291
benzoic acid	high	344	589	914	344	496	624
o-hydroxybenzoic acid	low	0.2	0.4	0.6	0.2	0.3	0.4
o-hydroxybenzoic acid	medium	-	-	-	-	-	-
o-hydroxybenzoic acid	high	29	50	78	29	40	53
p-hydroxybenzoic acid	low	4	8	12	4	6	8
p-hydroxybenzoic acid	medium	9	15	24	9	12	16
p-hydroxybenzoic acid	high	50	85	132	50	68	90
vanillic acid	low	45	77	120	45	62	82
vanillic acid	medium	-	-	-	-	-	-
vanillic acid	high	705	1207	1873	705	962	1278
syringic acid	low	8	14	21	8	11	14
syringic acid	medium	-	-	-	-	-	-
syringic acid	high	17	29	45	17	23	31

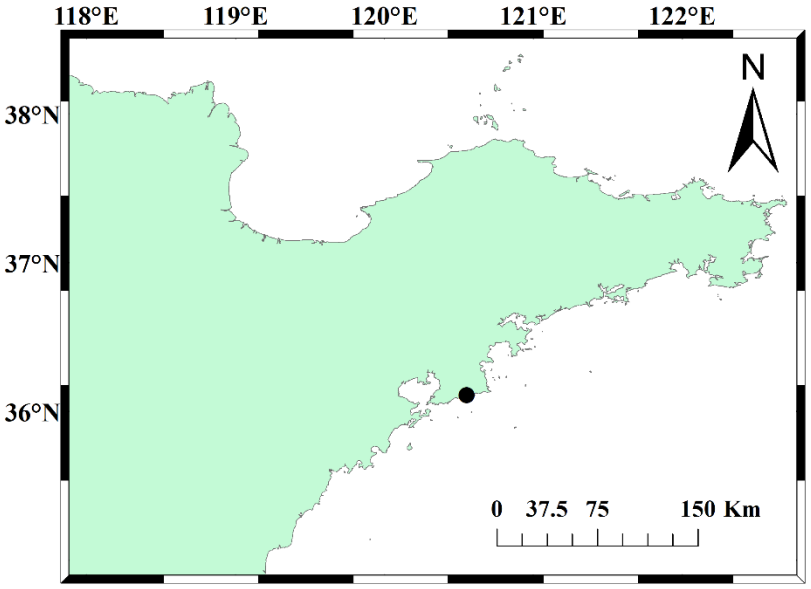

Fig. S1. Sampling site at Shazikou along the Yellow Sea coast, Qingdao, China.

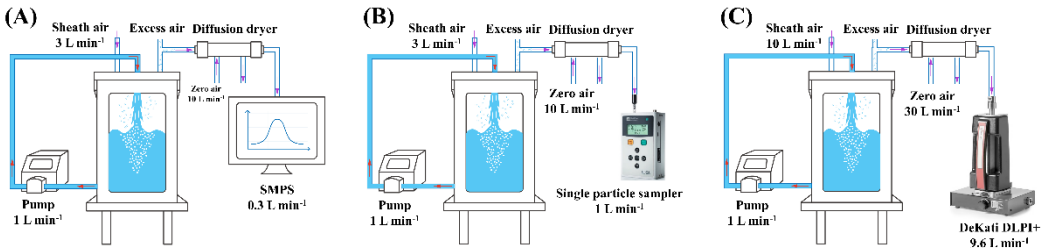

Fig. S2. Schematic picture of the plunging jet-sea spray aerosol generator: SMPS sampling (A), single particle sampling (B), and DeKati DLPI+ sampling (C). The red arrows represent the flow direction of seawater, and the purple arrows represent the flow of gases and aerosol particles.

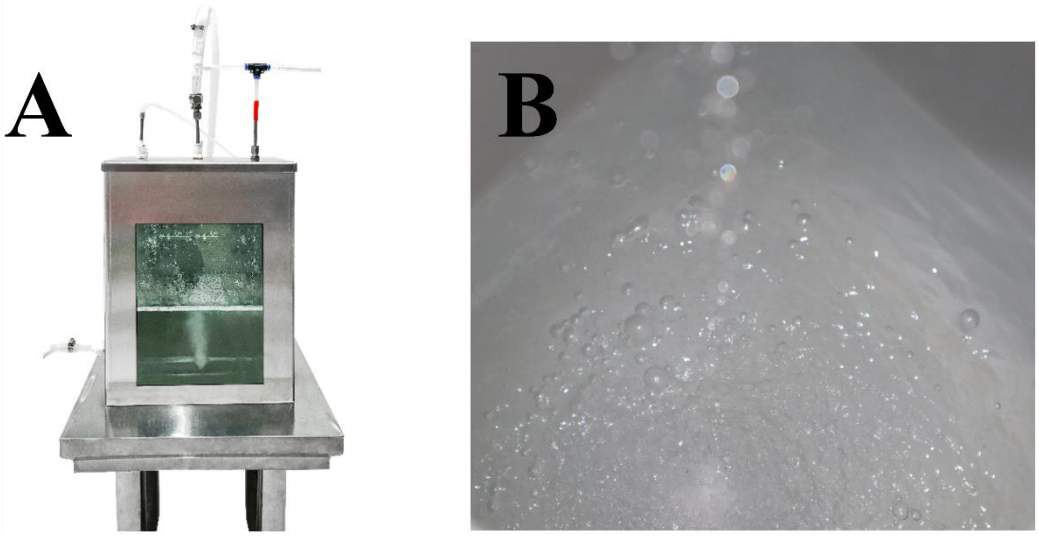

Fig. S3. Physical diagram of the SSA simulation chamber (A) and the top view of the bubble generation in the chamber (B).

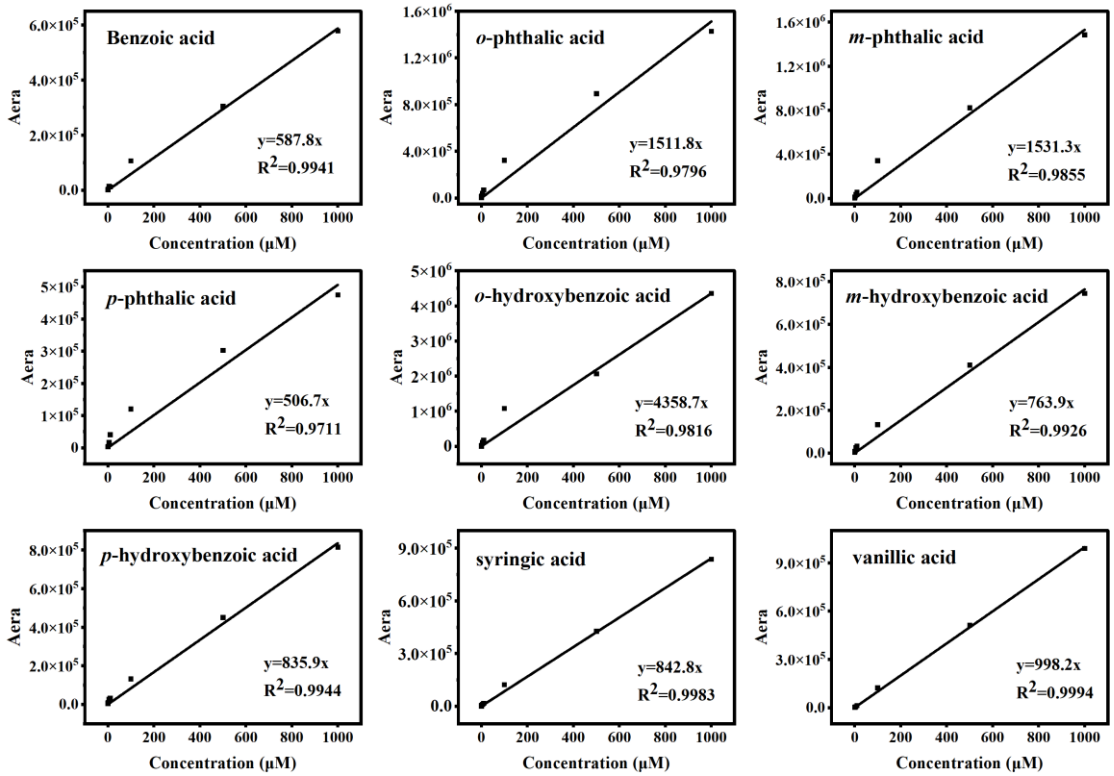

Fig. S4. Standard curves for aromatic acids were constructed within a concentration range of 0.01–1000 μM, with more than seven data points.

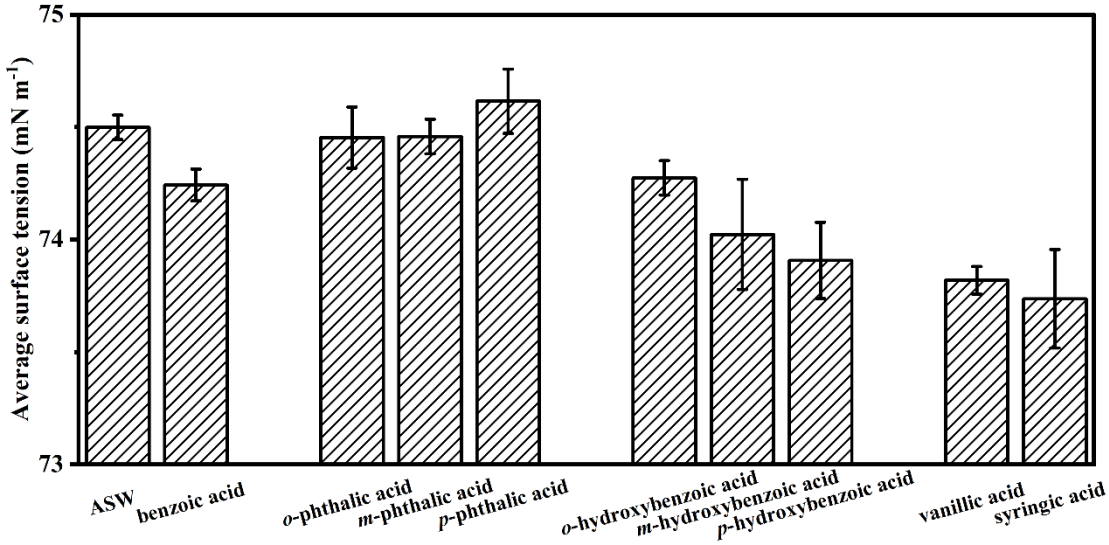

Fig. S5. Measured surface tension values of artificial seawater (ASW) and aromatic acid-containing ASW.

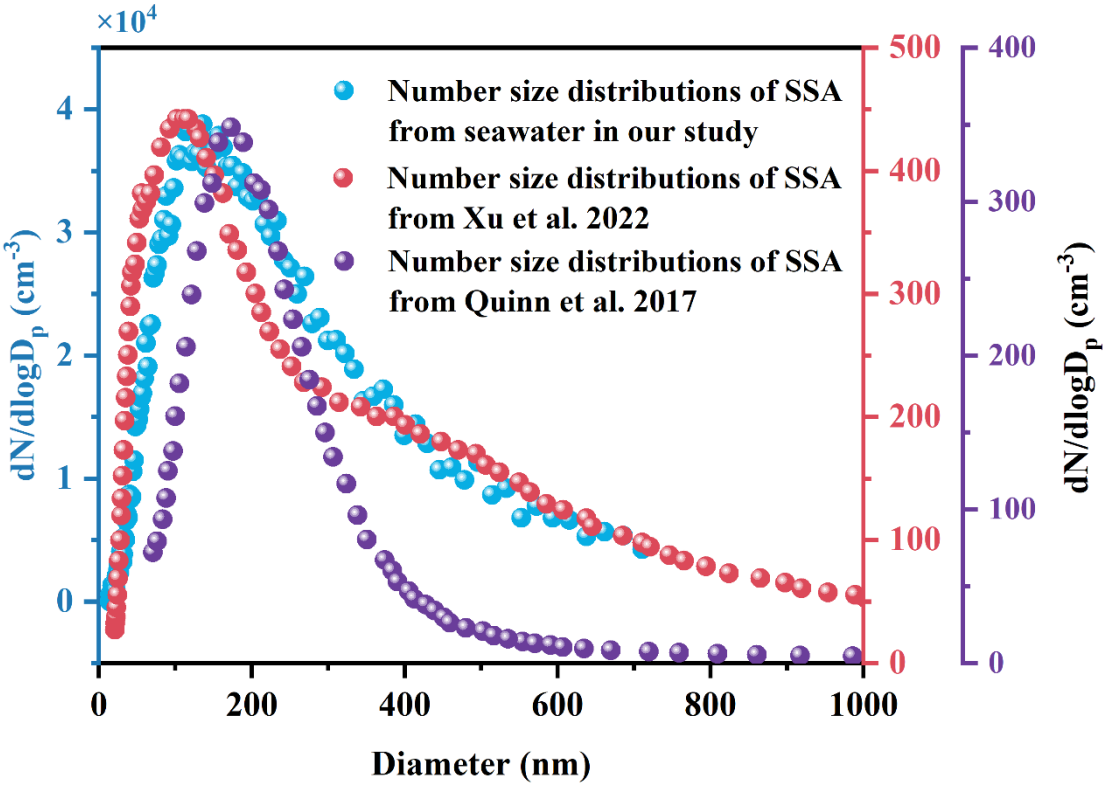

Fig. S6. Number size distribution of SSA generated with the SSA simulation chamber in this study compared with field studies.

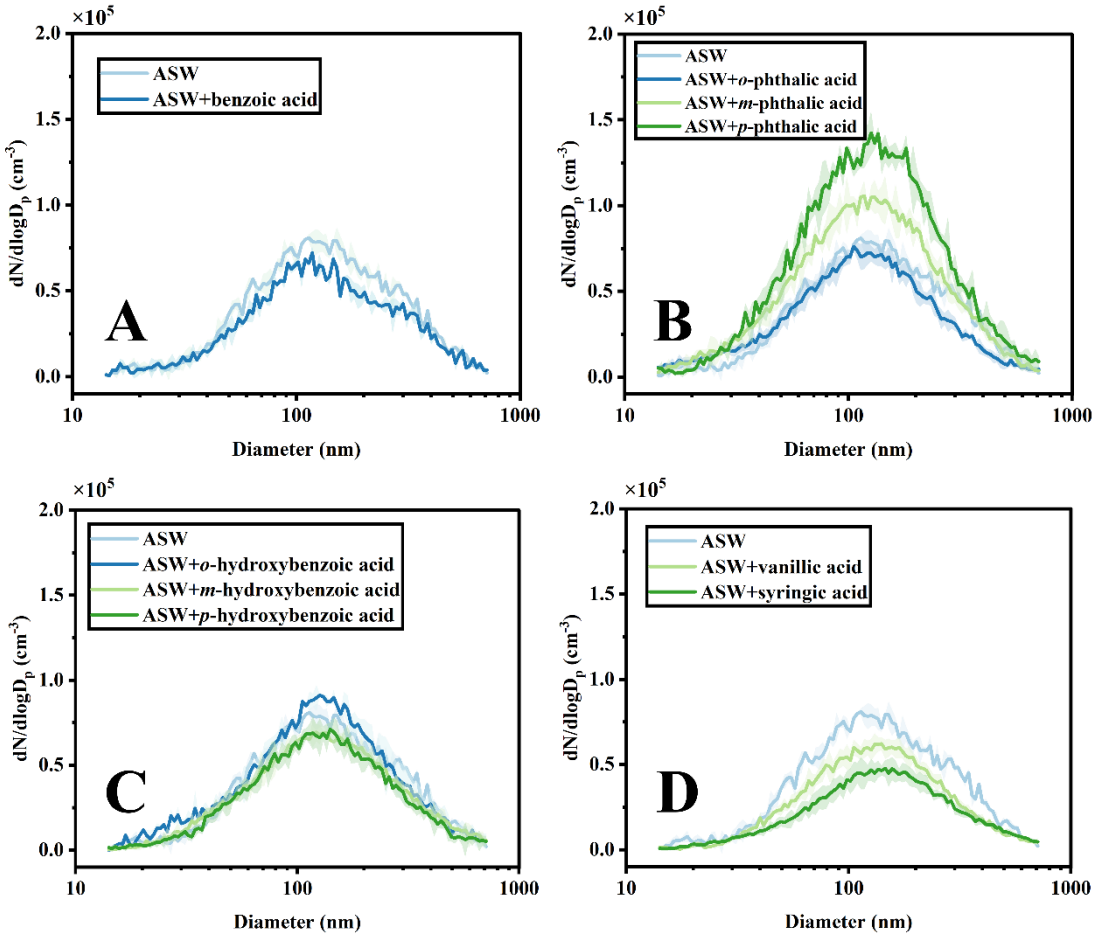

Fig. S7. Number concentration distribution of sea salt particles and SSA particles containing benzoic acids (A), benzenedicarboxylic acids (B), hydroxybenzoic acids (C), vanillic acid and syringic acid (D). ASW represents artificial seawater.

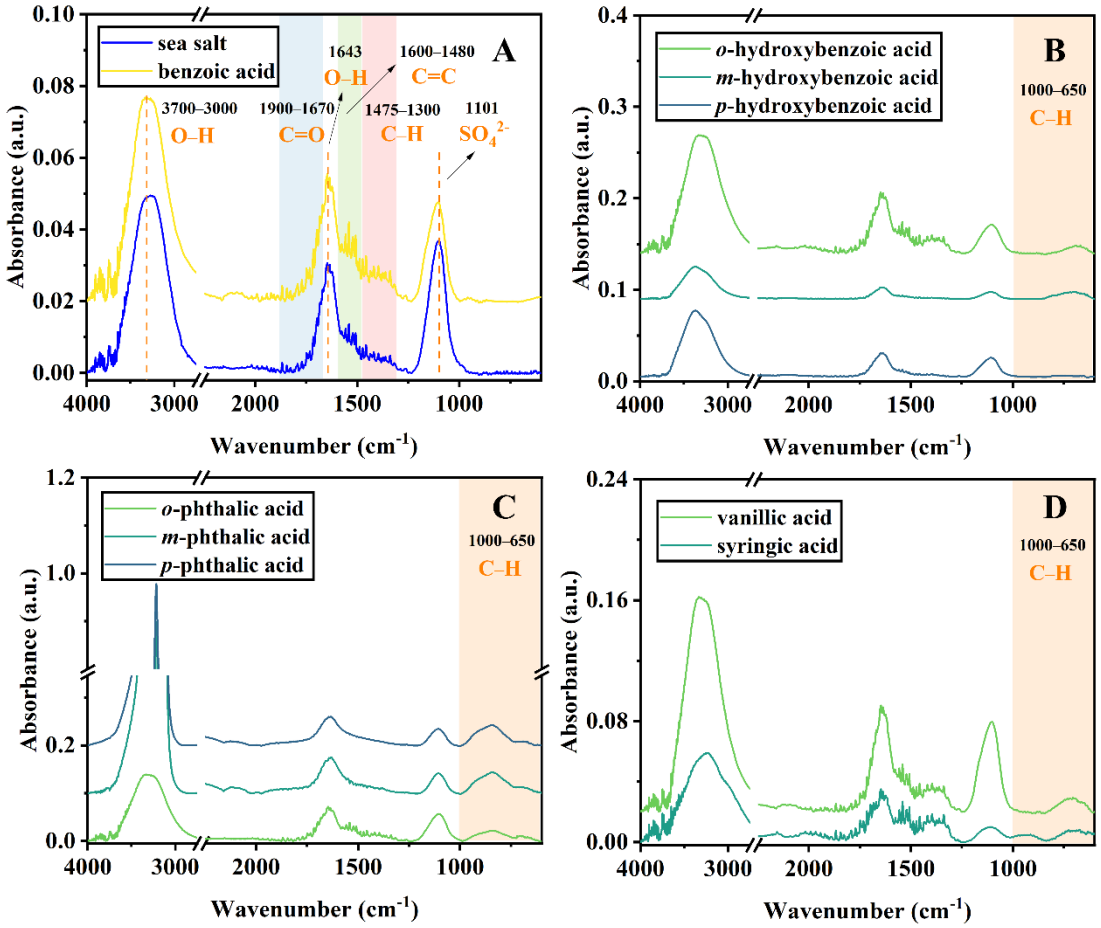

Fig. S8. Infrared spectra of aromatic acids-containing sea spray aerosol particles generated from SSA generation chamber. The ATR-FTIR data from the 2750–2250 cm^{-1} region, where CO_2 peaks are present, were not shown for clarity.

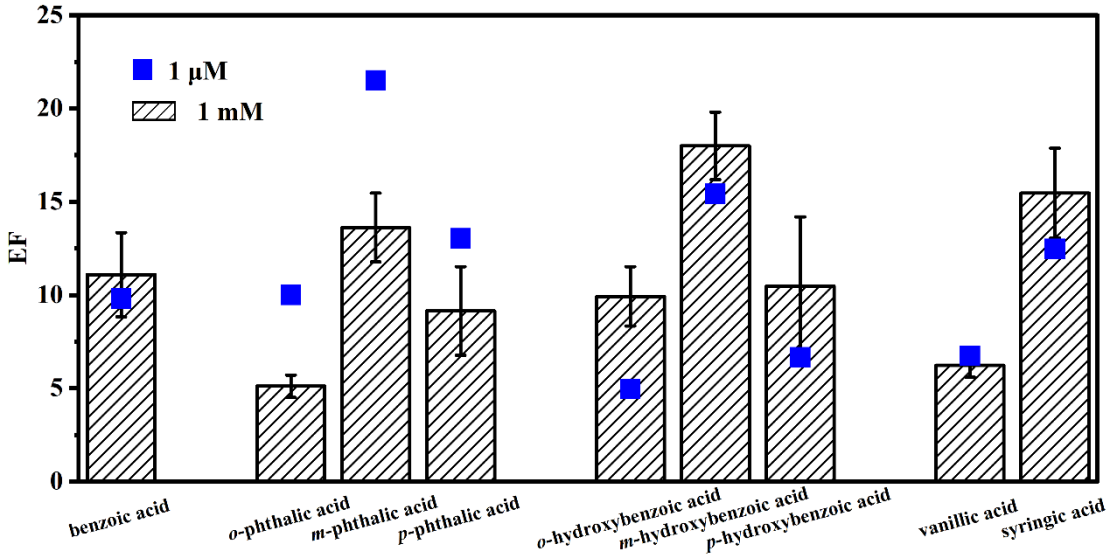

Fig. S9. Enrichment factors of aromatic acids at different concentrations from artificial seawater to the atmosphere.

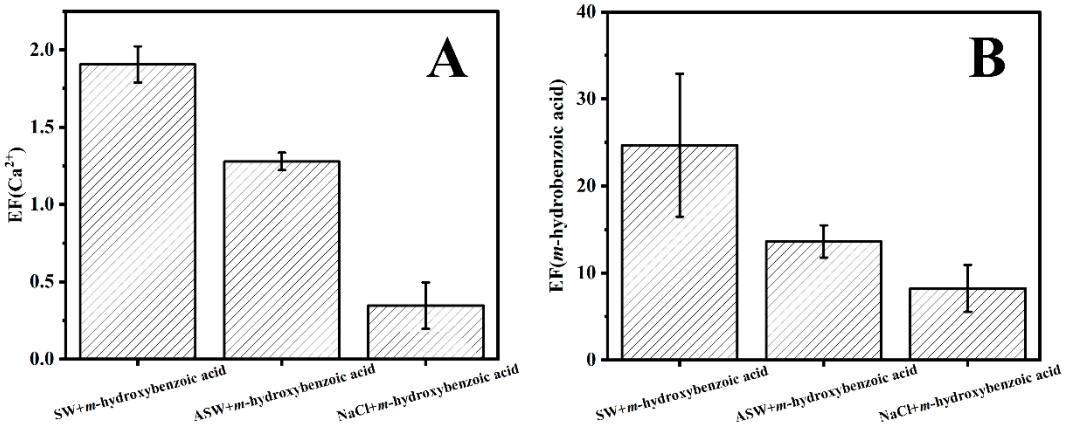

Fig. S10. Enrichment factors of Ca^{2+} and *m*-hydroxybenzoic acid in submicron SSA with seawater (SW), artificial seawater (ASW), and NaCl solution.

References

Abdel-Hamid A. Hamdy, N. M. E.-f., A. El-Beih, M. Mohammed, W. Mettwally: Egyptian red sea seagrass as a source of biologically active secondary metabolites, Egyptian Pharmaceutical Journal 19, 224, 10.4103/epj.epj_57_19, 2020.

Al-Zereini, W., Fotso Fondja Yao, C. B., Laatsch, H., and Anke, H.: Aqabamycins A-G: novel nitro maleimides from a marine Vibrio species. I. Taxonomy, fermentation, isolation and biological activities, J. Antibiot., 63, 297–301, 10.1038/ja.2010.34, 2010.

Alygizakis, N. A., Gago-Ferrero, P., Borova, V. L., Pavlidou, A., Hatzianestis, I., and Thomaidis, N. S.: Occurrence and spatial distribution of 158 pharmaceuticals, drugs of abuse and related metabolites in offshore seawater, Sci. Total Environ., 541, 1097–1105, 10.1016/j.scitotenv.2015.09.145, 2016.

Boreddy, S. K. R., Hegde, P., Arun, B. S., Aswini, A. R., and Babu, S. S.: Molecular composition and light-absorbing properties of organic aerosols from west-coast of tropical India, Sci. Total Environ., 845, 157163, 10.1016/j.scitotenv.2022.157163, 2022.

Boreddy, S. K. R., Mochizuki, T., Kawamura, K., Bikkina, S., and Sarin, M. M.: Homologous series of low molecular weight (C1-C10) monocarboxylic acids, benzoic acid and hydroxyacids in fine-mode (PM2.5) aerosols over the Bay of Bengal: Influence of heterogeneity in air masses and formation pathways, Atmos. Environ., 167, 170–180, 10.1016/j.atmosenv.2017.08.008, 2017.

Castillo, A., Celeiro, M., Lores, M., Grgić, K., Banožić, M., Jerković, I., and Jokić, S.: Bioprospecting of Targeted Phenolic Compounds of Dictyota dichotoma, Gongolaria barbata, Ericaria amentacea, Sargassum hornschuchii and Ellisolandia elongata from the Adriatic Sea Extracted by Two Green Methods, Mar. Drugs, 21, 97, 10.3390/md21020097, 2023.

Cuadros-Orellana, S., Pohlschröder, M., and Durrant, L. R.: Isolation and characterization of halophilic archaea able to grow in aromatic compounds, Int. Biodeterior. Biodegradation, 57, 151–154, 10.1016/j.ibiod.2005.04.005, 2006.

Deshmukh, D. K., Kawamura, K., Lazaar, M., Kunwar, B., and Boreddy, S. K. R.: Dicarboxylic acids, oxoacids, benzoic acid, α-dicarbonyls, WSOC, OC, and ions in spring aerosols from Okinawa Island in the western North Pacific Rim: size distributions and formation processes, Atmos. Chem. Phys., 16, 5263–5282, 10.5194/acp-16-5263-2016, 2016.

Di Giacinto, F., Di Renzo, L., Mascilongo, G., Notarstefano, V., Gioacchini, G., Giorgini, E., Bogdanović, T., Petričević, S., Listeš, E., Brkljača, M., Conti, F., Profico, C., Zambuchini, B., Di Francesco, G., Giansante, C., Diletti, G., Ferri, N., and Berti, M.: Detection of microplastics, polymers and additives in edible muscle of swordfish (Xiphias gladius) and bluefin tuna (Thunnus thynnus) caught in the Mediterranean Sea, J. Sea Res., 192, 102359, 10.1016/j.seares.2023.102359, 2023.

Di Renzo, L., Mascilongo, G., Berti, M., Bogdanović, T., Listeš, E., Brkljača, M., Notarstefano, V., Gioacchini, G., Giorgini, E., Olivieri, V., Silvestri, C., Matiddi, M., D'Alterio, N., Ferri, N., and Di Giacinto, F.: Potential impact of microplastics and additives on the health status of loggerhead turtles (Caretta caretta) stranded along the central adriatic coast, Water Air Soil Pollut., 232, 98, 10.1007/s11270-021-04994-8, 2021.

Ding, Z., Du, W., Wu, C., Cheng, C., Meng, J., Li, D., Ho, K., Zhang, L., and Wang, G.: Summertime atmospheric dicarboxylic acids and related SOA in the background region of Yangtze River Delta, China: Implications for heterogeneous reaction of oxalic acid with sea salts, Sci. Total Environ., 757, 143741, 10.1016/j.scitotenv.2020.143741, 2021.

Fisch, K., Waniek, J. J., and Schulz-Bull, D. E.: Occurrence of pharmaceuticals and UV-filters in riverine run-offs and waters of the German Baltic Sea, Mar. Pollut. Bull., 124, 388–399, 10.1016/j.marpolbul.2017.07.057, 2017.

Fotso Fondja Yao, C. B., Zereini, W. A., Fotso, S., Anke, H., and Laatsch, H.: Aqabamycins A–G: novel nitro maleimides from a marine Vibrio species: II. Structure elucidation*, J. Antibiot., 63, 303–308, 10.1038/ja.2010.35, 2010.

Gliss, J., Mortier, A., Schulz, M., Andrews, E., Balkanski, Y., Bauer, S. E., Benedictow, A. M. K., Bian, H., Checa-Garcia, R., Chin, M., Ginoux, P., Griesfeller, J. J., Heckel, A., Kipling, Z., Kirkevåg, A., Kokkola, H., Laj, P., Sager, P. L., Lund, M. T., Myhre, C. L., Matsui, H., Myhre, G., Neubauer, D., Noije, T. v., North, P., Olivié, D. J. L., Rémy, S., Sogacheva, L., Takemura, T., Tsigaridis, K., and Tsyro, S. G.: AeroCom phase III multi-model evaluation of the aerosol life cycle and optical properties using ground- and space-based remote sensing as well as surface in situ observations, Atmos. Chem. Phys., 21, 87–128, 10.5194/acp-21-87-2021, 2021.

Hawas, U. W. and Abou El-Kassem, L. T.: Thalassiolin D: a new flavone O-glucoside Sulphate from the seagrass Thalassia hemprichii, Nat. Prod. Res., 31, 2369–2374, 10.1080/14786419.2017.1308367, 2017.

Hu, J., Loh, P. S., Chang, Y.-P., and Yang, C.-W.: Multi-proxy records of paleoclimatic changes in sediment core ST2 from the southern Zhejiang-Fujian muddy coastal area since 1650 yr BP, Cont Shelf

Res, 239, 104717, 10.1016/j.csr.2022.104717, 2022.
Jingchuan Xue, N. S., Madhavan Elangovan, Guthrie Diamond, Kurunthachalam Kannan: Elevated accumulation of parabens and their metabolites in marine mammals from the United States coastal waters, Environ. Sci. Technol., 49, 12071–12079, 2015.
Kawamur, B. K. a. K.: Seasonal distributions and sources of low molecular weight dicarboxylic acids, ωoxocarboxylic acids, pyruvic acid, α-dicarbonyls and fatty acids in ambient aerosols from subtropical Okinawa in the western Pacific Rim, Environ. Chem., 11, 673–689, 10.1071/EN14097_AC, 2014.
Klejdus, B., Plaza, M., Šnóblová, M., and Lojková, L.: Development of new efficient method for isolation of phenolics from sea algae prior to their rapid resolution liquid chromatographic–tandem mass spectrometric determination, J. Pharm. Biomed. Anal., 135, 87–96, 10.1016/j.jpba.2016.12.015, 2017.
Liao, C. and Kannan, K.: Temporal trends of parabens and their metabolites in mollusks from the Chinese Bohai Sea during 2006–2015: Species-specific accumulation and implications for human exposure, Environ. Sci. Technol., 52, 9045–9055, 10.1021/acs.est.8b02750, 2018.
Liao, C., Shi, J., Wang, X., Zhu, Q., and Kannan, K.: Occurrence and distribution of parabens and bisphenols in sediment from northern Chinese coastal areas, Environ. Pollut., 253, 759–767, 10.1016/j.envpol.2019.07.076, 2019.
Liu, S., Longnecker, K., Kujawinski, E. B., Vergin, K., Bolaños, L. M., Giovannoni, S. J., Parsons, R., Opalk, K., Halewood, E., Hansell, D. A., Johnson, R., Curry, R., and Carlson, C. A.: Linkages among dissolved organic matter export, dissolved metabolites, and associated microbial community structure response in the Northwestern Sargasso Sea on a seasonal scale, Front. Microbiol., 13, 833252, 10.3389/fmicb.2022.833252, 2022.
Lu, S., Lin, C., Lei, K., Xin, M., Wang, B., Ouyang, W., Liu, X., and He, M.: Endocrine-disrupting chemicals in a typical urbanized bay of Yellow Sea, China: Distribution, risk assessment, and identification of priority pollutants, Environ. Pollut., 287, 117588, 10.1016/j.envpol.2021.117588, 2021.
Lu, S., Wang, J., Wang, B., Xin, M., Lin, C., Gu, X., Lian, M., and Li, Y.: Comprehensive profiling of the distribution, risks and priority of pharmaceuticals and personal care products: A large-scale study from rivers to coastal seas, Water Res., 230, 119591, 10.1016/j.watres.2023.119591, 2023.
Martí-Quijal, F. J., Tornos, A., Príncep, A., Luz, C., Meca, G., Tedeschi, P., Ruiz, M.-J., and Barba, F. J.: Impact of fermentation on the recovery of antioxidant bioactive compounds from sea bass byproducts, Antioxidants, 9, 239, 10.3390/antiox9030239, 2020.
Mochizuki, T., Kawamura, K., Aoki, K., and Sugimoto, N.: Long-range atmospheric transport of volatile monocarboxylic acids with Asian dust over a high mountain snow site, central Japan, Atmos. Chem. Phys., 16, 14621–14633, 10.5194/acp-16-14621-2016, 2016.
mostafa, s., Mohamed, H., Ibraheem, I., and Abdel-Raouf, N.: Controlling of microbial growth by using cystoseira barbata extract, Egypt. J. Bot., 57, 469–477, 10.21608/ejbo.2017.911.1071, 2017.
Poznyakovsky, V., Kalenik, T., Wojciech, P., Tabakaeva, O., and Tabakaev, A.: Antioxidant properties of edible sea weed from the Northern Coast of the Sea of Japan, Foods Raw Mater., 9, 262–270, 10.21603/2308-4057-2021-2-262-270, 2021.
Quinn, P. K., Collins, D. B., Grassian, V. H., Prather, K. A., and Bates, T. S.: Chemistry and related properties of freshly emitted sea spray aerosol, Chem. Rev., 115, 4383–4399, 10.1021/cr500713g, 2015.
Ren, L., Weng, L., Chen, D., Hu, H., Jia, Y., and Zhou, J. L.: Bioremediation of PAEs-contaminated saline soil: The application of a marine bacterial strain isolated from mangrove sediment, Mar. Pollut. Bull., 192, 115071, 10.1016/j.marpolbul.2023.115071, 2023.
Rukachaisirikul, V., Khamthong, N., Sukpondma, Y., Phongpaichit, S., Hutadilok-Towatana, N., Graidist, P., Sakayaroj, J., and Kirtikara, K.: Cyclohexene, diketopiperazine, lactone and phenol derivatives from the sea fan-derived fungi Nigrospora sp. PSU-F11 and PSU-F12, Arch. Pharm. Res., 33, 375–380, 10.1007/s12272-010-0305-3, 2010.
Sanjuan, O. N., Sait, S. T. L., Gonzalez, S. V., Tomas, J., Raga, J. A., and Asimakopoulos, A. G.: Phthalate metabolites in loggerhead marine turtles (Caretta caretta) from the Mediterranean Sea (East Spain region), Environ. Toxicol. Chem., 5, 178–185, 10.1016/j.enceco.2023.08.003, 2023.
Shao, C., Guo, Z., Peng, H., Peng, G., Huang, Z., She, Z., Lin, Y., and Zhou, S.: A new isoprenyl phenyl ether compound from mangrove fungus, Chem Nat Compd, 43, 377–380, 10.1007/s10600-007-0142-x, 2007.
Shumilina, E., Skavang, P. K., and Dikiy, A.: Application of NMR spectroscopy for the detection and quantification of phthalic acid in fish muscles: The case of Atlantic Cod from Norwegian Sea, Mar. Environ. Res., 188, 105973, 10.1016/j.marenvres.2023.105973, 2023.
Simoneit, B. R. T.: Biomass burning- a review of organic tracers for smoke from incomplete combustion, Appl. Geochem., 17, 129–162, 10.1016/S0883-2927(01)00061-0, 2022.
Textor, C., Schulz, M., Guibert, S., Kinne, S., Balkanski, Y., Bauer, S., Berntsen, T., Berglen, T., Boucher, O., Chin, M., Dentener, F., Diehl, T., Easter, R., Feichter, H., Fillmore, D., Ghan, S., Ginoux, P., Gong,

S., Grini, A., Hendricks, J., Horowitz, L., Huang, P., Isaksen, I., Iversen, T., Kloster, S., Koch, D., Kirkevag, A., Kristjansson, J. E., Krol, M., Lauer, A., Lamarque, J. F., Liu, X., Montanaro, V., Myhre, G., Penner, J., Pitari, G., Reddy, S., Seland, Stier, P., Takemura, T., and Tie, X.: Analysis and quantification of the diversities of aerosol life cycles within AeroCom, Atmos. Chem. Phys., 6, 1777–1813, 10.5194/acp-6-1777-2006, 2006.
Tian, M., Zhu, T., Park, H. E., and Row, K. H.: Purification of 4-hydroxybenzoic acid and 4-hydroxybenzaldehyde from Laminaria japonica aresch using commercial and monolithic sorbent in SPE cartridge, Anal. Lett., 45, 2359–2366, 10.1080/00032719.2012.691590, 2012.
Wang, J., Yao, P., Bianchi, T. S., Li, D., Zhao, B., Cui, X., Pan, H., Zhang, T., and Yu, Z.: The effect of particle density on the sources, distribution, and degradation of sedimentary organic carbon in the Changjiang Estuary and adjacent shelf, Chem. Geol., 402, 52–67, 10.1016/j.chemgeo.2015.02.040, 2015.
Xu, F., Jin, H., Ji, Z., Chen, J., and Loh, P. S.: Sources and distribution of sedimentary organic matter along the northern Bering and Chukchi Seas, J Environ Sci (China), 52, 66–75, 10.1016/j.jes.2016.04.003, 2017.
Yang, J., Zhao, W., Wei, L., Zhang, Q., Zhao, Y., Hu, W., Wu, L., Li, X., Pavuluri, C. M., Pan, X., Sun, Y., Wang, Z., Liu, C.-Q., Kawamura, K., and Fu, P.: Molecular and spatial distributions of dicarboxylic acids, oxocarboxylic acids, and α-dicarbonyls in marine aerosols from the South China Sea to the eastern Indian Ocean, Atmos. Chem. Phys., 20, 6841–6860, 10.5194/acp-20-6841-2020, 2020.
Zangrando, R., Corami, F., Barbaro, E., Grosso, A., Barbante, C., Turetta, C., Capodaglio, G., and Gambaro, A.: Free phenolic compounds in waters of the Ross Sea, Sci. Total Environ., 650, 2117–2128, 10.1016/j.scitotenv.2018.09.360, 2019.
Zhao, X., Qiu, W., Zheng, Y., Xiong, J., Gao, C., and Hu, S.: Occurrence, distribution, bioaccumulation, and ecological risk of bisphenol analogues, parabens and their metabolites in the Pearl River Estuary, South China, Ecotoxicol. Environ. Saf., 180, 43–52, 10.1016/j.ecoenv.2019.04.083, 2019.
Zhou, X., Lin, X., Guo, X., Yang, B., Yang, X.-W., and Liu, Y.: Chemical constituents of the sponge mycale species from South China Sea, Rec. Nat. Prod., 7, 119–123, 2013.
Zhu, Y., Tilgner, A., Hoffmann, E. H., Herrmann, H., Kawamura, K., Xue, L., Yang, L., and Wang, W.: Molecular distributions of dicarboxylic acids, oxocarboxylic acids, and α-dicarbonyls in aerosols over Tuoji Island in the Bohai Sea: Effects of East Asian continental outflow, Atmos Res, 272, 106154, 10.1016/j.atmosres.2022.106154, 2022.